Gábor Transform-Based Antibody Quantitation in Serum: An Inter-Laboratory Liquid Chromatography/High-Resolution Mass Spectrometry Investigation

Kayd L. Meldrum[1], Andrew K. Swansiger[1], Jacob Koscho[1], Lily Miller[1], John Sausen[2], Anthony D. Maus[3], Paula M. Ladwig[3], Maria A. V. Willrich[3], James S. Prell[1,4,*]

[1]Department of Chemistry and Biochemistry, 1253 University of Oregon, Eugene, OR 97403-1253, USA

[2]Agilent Technologies, Inc., 5301 Stevens Creek Blvd., Santa Clara, CA 95051, USA

[3]Department of Laboratory Medicine and Pathology, Mayo Clinic, 200 First Street SW, Rochester, MN 55905, USA

[4]Materials Science Institute, 1252 University of Oregon, Eugene, OR 97403-1252, USA

Submitted to *Analytical Chemistry*

21 August 2024

[*]Corresponding author email: jprell@uoregon.edu

Keywords: mass spectrometry, monoclonal antibody, quantitation, Gábor transform, Fourier transform

Abstract

Therapeutic monoclonal antibodies (t-mAbs) are crucial for treating various conditions, including cancers and autoimmune disorders. Accurate quantitation and pharmacokinetic monitoring of t-mAbs in serum is essential, but current methods like ligand binding assays (LBAs) and bottom-up peptide liquid chromatography-tandem mass spectrometry (LC-MS/MS) can lack the sensitivity and specificity needed to meet clinical demands. Emerging techniques using high-resolution mass spectrometry (HRMS) in top-down and middle-up approaches offer improved ability to accurately quantify mAb proteoforms apart from degradation products by keeping the sample proteins intact or minimizing digestion. This study describes the first use of Gábor Transform- (GT-) based iFAMS Quant+ software to quantify a t-mAb (vedolizumab) from ~400 samples using an Agilent 6545XT AdvanceBio Q-TOF at University of Oregon. These results are compared to a previously validated Laboratory Developed Test (LDT) from Mayo Clinic utilizing a Thermo Q Exactive Plus Orbitrap. The Mayo method used conventional extracted ion chromatograms (XICs) of select charge states for quantitation, while the iFAMS Quant+ method utilized GT-based charge state deconvolution, background subtraction, and signal integration. Calibration and quality control (QC) analyses and Passing-Bablok regression of 351 subject samples demonstrated excellent agreement between the two methods. The iFAMS Quant+ workflow exhibited unique advantages for characterizing interferents and analyte signal anomalies due to its deconvolution-based approach.

Introduction

Therapeutic monoclonal antibodies (t-mAbs) have become an extremely important branch of pharmaceuticals used to treat a range of conditions including cancers and autoimmune disorders.[1–6] Many of these treatments benefit from therapeutic drug monitoring (TDM), which guides dosage adjustments and has been shown to improve treatment outcome.[7–9] However, current clinical quantitation approaches—such as ligand binding assays (LBAs) and bottom-up, peptide liquid chromatography tandem mass spectrometry (LC-MS/MS) assays have limitations in terms of the ability to discriminate between related proteoforms, aggregates, pre-digestion degradation products, as well as being prone to interference from polyclonal immunoglobulins present in patient serum samples.[10–15] To improve specificity and sensitivity, emerging studies have explored methods measuring the intact proteins—or subunits of them, such as antibody light chains, prepared by chemical reduction—using high resolution mass spectrometry (HRMS) coupled with liquid chromatography (LC) in top-down, middle-up, and middle-down approaches.[15–23]

The improved resolution and quadrupole transmission of modern HRMS is useful for characterizing intact proteins as large as t-mAbs. Most LC-HRMS methods use electrospray ionization (ESI) to gently introduce the proteins to the gas phase. However, ESI spreads each protein signal across multiple charge states, reducing the signal-to-noise for individual charge states, and this phenomenon can often lead to highly congested mass spectra, especially for biological samples such as t-mAbs in serum.[24] The charge distribution is also sensitive to experimental conditions such as pH and can drift over time.[25,26] How best to analyze mass spectral signal spread across a charge distribution is an ongoing topic of study, with the two main

approaches at present being direct integration via extracted ion chromatograms (XICs) and mass spectrum deconvolution.[17,27–29]

For approaches using XICs, typically a few charge states for each analyte are selected based on their relatively high abundance, robustness to experimental drift, and lack of overlapping interferent peaks to use as representatives of the whole analyte distribution. An XIC is generated from the addition of these representative charge states, and the chromatographic peak for the analyte is integrated for quantitation after automatic baseline determination. An example of this method was validated as a Laboratory Developed Test (LDT) and published by Cradic et al. from Mayo Clinic.[16] Briefly, the Mayo method uses a surrogate protein internal standard, reductive cleavage of the t-mAb light chains, and liquid chromatography in combination with high-resolution accurate mass MS to generate XICs from addition of select charge states for quantitation.

Deconvolution algorithms, including Maximum Entropy, PMI Intact from Protein Metrics, UniDec, THRASH, and iFAMS,[30–34] aim to utilize all or many charge states to generate a combined mass spectrum with improved signal-to-noise relative to an individual charge state. Although deconvolved mass spectra are most often used for analyte characterization such as accurate mass and proteoform or ligand identification, some recent studies have demonstrated quantitative workflows from deconvolution despite past wariness regarding accuracy and precision.[17,19,20,28,29,35–37] Although many different types of deconvolution algorithms exist, currently, there are no open-source, vendor-neutral deconvolution software packages that offer clinically-validated, automated protein quantitation primarily due to the fact that the deconvolved mass spectra produced in many available software packages can be highly dependent on user-defined parameters.[24] Moreover, to ensure the reproducibility and traceability necessary for

routine clinical applications, there is a need for robust deconvolution protocols that can be standardized and automated with minimal user involvement.[22,38]

iFAMS (interactive Fourier-Transform Analysis for Mass Spectrometry) is an in-house developed, open-source mass spectrum deconvolution algorithm that uses Gábor Transform (GT) to separate, filter, and deconvolve ion signals based on both their *m*/*z* and frequency (i.e., local periodic peak spacings in the mass spectrum due to isotopologs, ligand-binding states, post-translational modifications, etc.).[34,39–42] Although originally developed for qualitative analysis of complex, highly congested mass spectra via Fourier Transform (FT)-based deconvolution, iFAMS now includes numerous additional FT-based tools, such as macromolecular defect analysis, theoretical isotope distribution calculation, and automatic mass spectral signal detection and background subtraction. The latest version (iFAMS Quant) was developed with additional tools for intact protein analysis and was described in detail in a previous publication; however, quantitation using iFAMS Quant (or GT algorithms in general) has never been compared against other benchmark MS-based quantitative analysis workflows.[42]

In this article, we demonstrate the precision, accuracy, and advantages of iFAMS Quant+, a licensable version of iFAMS Quant with the ability to interact directly with Agilent ".d" LC/MS data files. T-mAb quantitation results using an Agilent 6545XT AdvanceBio Q-TOF mass spectrometer in combination with iFAMS Quant+ are compared to results from the validated Mayo method using a Thermo Q Exactive Plus Orbitrap mass spectrometer. Excellent agreement is obtained between the methods for quantitation of subject samples presenting for TDM despite using different instrumentation and a freeze-ship-thaw step for the extracted standards, quality control (QC), and samples. We further show the unique capabilities of the GT-based iFAMS Quant+ method to reveal interferents with nearly identical mass to the analyte of

interest that can pose challenges for quantitation. Finally, effects of the freeze-ship-thaw step and sample degradation over time are highlighted that serve as caveats for inter-laboratory biomolecule quantitation studies more broadly.

Experimental Methods

Reagents. Dithiothreitol (DTT) and ammonium bicarbonate were purchased from Sigma-Aldrich (St. Louis, MO, USA). Melon™ Gel was purchased from Thermo Fisher Scientific (Waltham, MA, USA). Normal human serum (NHS) was purchased from MilliporeSigma (Burlington, MA, USA). Vedolizumab (Entyvio; Takeda Pharmaceuticals) and nivolumab (Opdivo; Bristol Myers Squibb) were purchased from Mayo Clinic pharmacy. Solvents used by Mayo Clinic were high-performance liquid chromatography (HPLC) grade acetonitrile, isopropyl alcohol, and clinical grade laboratory water (CLRW) (each from MilliporeSigma; Burlington, MA, USA); and formic acid (Thermo Fisher Scientific; Walthham, MA, USA).[16] Solvents used by the University of Oregon lab were ultrapure (18 MΩ·cm) water prepared using a Barnstead E-Pure Ultrapure Water Purification System (Thermo Fisher Scientific; Waltham, MA, USA), liquid chromatography-mass spectrometry (LC-MS) grade acetonitrile, LC-MS grade isopropyl alcohol, and puriss. p.a. grade formic acid (each from Sigma-Aldrich; St. Louis, MO, USA).

Sample preparation. Vedolizumab was initially diluted to 15 mg/mL in CLRW followed by further dilution to make intermediate stocks in NHS (10 mg/mL and 1 mg/mL) for spiking standards in NHS for an analytical measuring interval from 2 to 200 mcg/mL. The surrogate internal standard (IS), nivolumab, was diluted to 75 µg/mL in Melon™ Gel Buffer solution. Stocks were stored at −20 °C. The working IS was refrigerated at 2-8 °C. Three hundred microliters of Melon™ Gel slurry was added to a 0.2-µm polyvinylidene fluoride (PVDF) filter

plate (Sigma-Aldrich; St. Louis, MO, USA) affixed to a deep well collection plate. 30 µL of standards, QC and patients were added to respective wells. 30 µL of IS was added to each well and the plate incubated on an orbital mixer (500 rpm or 4 g) at room temperature for 30 minutes. The eluate was pushed to the collection plate using positive pressure. 100 mM DTT solution was prepared in 50 mM ammonium bicarbonate and 250 µL of this solution was added to each well of the collection plate. Samples were incubated in a rocking incubator at 55 °C for 30 minutes to reduce the disulfide bonds between the light and heavy chains of the immunoglobulins. Additional details on the sample preparation method are described elsewhere.[16]

Samples were enriched and analyzed at Mayo Clinic. After this initial measurement, the 96 well plates were frozen and shipped to University of Oregon on dry ice (-78°C). Once received, the samples were thawed in a water bath of 23 °C for an hour, pipet mixed three times using a Rainn Liquidator 96 pipettor set for 105 µL, then immediately analyzed by LC/MS. Each prepared plate contained standards and QC along with 79 samples of residual serum that were obtained from subjects treated with vedolizumab infusion therapy. Each plate contained a calibration series with nominal concentrations of 2, 5, 10, 25, 75, 125, and 200 µg/mL vedolizumab and two sets of 4 levels of QC with target concentrations of 6.8, 17.4, 48, and 146 µg/mL vedolizumab based on average concentrations from 20 previous runs at Mayo Clinic. In total, 5 plates were analyzed in this comparison. This study was reviewed and approved by the Institutional Review Board (IRB) (ID 14-009955) at Mayo Clinic.

Liquid Chromatography. Identical solvents, gradients, and columns were used at Mayo Clinic and University of Oregon, but the HPLC instruments were from different manufacturers. The Mayo Clinic lab used a Transcend™ TLX-4 UHPLC system in a multiplex configuration with three parallel columns running in a staggered fashion (Thermo Fisher Scientific; Waltham,

MA, USA), while the University of Oregon lab used a 1290 Infinity II LC system with only a single channel (Agilent Technologies; Santa Clara, CA, USA). The gradient consisted of an aqueous solvent of HPLC-grade or ultrapure water with 0.1% v/v formic acid and an organic solvent of 90% v/v acetonitrile, 9% v/v isopropyl alcohol, and 1% v/v formic acid. The gradient progresses from 10% to 98% organic solvent over the course of 11.5 minutes with 5.5 minutes of flushing and conditioning at a flow rate of 300 µL/min. A 10-µL sample injection was used on a 2.1 × 75 mm, 5-µm Poroshell 300SB-C3 reverse-phase column (Agilent Technologies; Santa Clara, CA, USA) heated to 60 °C. Detailed LC parameters can be found in the Supporting Information (Table S1).

High-resolution mass spectrometry. High-resolution accurate mass (HRAM) spectra were collected at the Mayo Clinic lab on a Q Exactive™ Plus Orbitrap MS (Thermo Fisher Scientific; Waltham, MA, USA) using a heated electrospray ion source (HESI) in positive mode. Mass accuracy was kept to less than 5 parts per million (ppm) drift over a run by running MS mass calibration (positive ion mode) before each run. Target resolution in profile mode was 140,000 FWHM at *m*/*z* 200. A full automatic gain control scan (AGC) was run with an *m*/*z* range of 1200-2500, ion count target of 10^6, and maximum injection time (IT) of 500 milliseconds. Then a targeted selection ion monitoring (t-SIM) was collected over the *m*/*z* range 1900-2400 with an AGC target of 2×10^5 and maximum IT of 125 milliseconds.[1] The full scan data was used for quantitation by deconvolution for this study, whereas the t-SIM is used for quantitation by XICs and reporting. Additional details for source parameters are included in the Supporting Information (Table S2).

At University of Oregon, HRAM spectra were collected using a 6545XT AdvanceBio quadrupole-time-of-flight (Q-TOF) mass spectrometer with the Dual Agilent Jet Stream

electrospray ionization (ESI) source (Agilent Technologies; Santa Clara, CA, USA). Spectra were acquired in positive ion, "high resolution" mode (4 GHz) over *m*/*z* range 1000-3200 with a target resolution of 50,000 FWHM at *m*/*z* 2722. Additional acquisition parameters are included in the Supporting Information (Table S3).

Data analysis. For data acquisition and analysis in the Mayo Clinic lab, TraceFinder version 4.1 (Thermo Fisher Scientific; Waltham, MA, USA) was used. From the t-SIM scan, the most abundant six isotope peaks (exact mass ±5 ppm) from three charge states (10+, 11+ and 12+) for the vedolizumab light chain were summed to produce the XIC used for quantitation of the analyte. The six most abundant isotope peaks for the +11 charge state for the nivolumab light chain were summed to produce the XIC for the IS used for correction, as previously described.[16] Figure 1a-e shows a schematic workflow for the Mayo method. XICs were manually reviewed before calibrating to a $1/x^2$-weighted quadratic curve (where x refers to calibrant concentration, and the weighting refers to individual squared-error contributions to the total squared error that is minimized in the least-squares fit).

For data analysis at the University of Oregon lab, iFAMS v. 6.3 (iFAMS Quant+) was used. Figure 1f-j shows a schematic workflow for the iFAMS Quant+ method. For each of the five data sets, a 0.3-minute retention time window was selected for MS extraction to span the majority of both the vedolizumab and nivolumab elution windows. GT spectrogram selections were made to include both the analyte and IS signal of identical charge states in a single box without using the automatic box re-optimization feature. The charge state range of 10-17+ was selected using the automated "Guided Search" tool in iFAMS Quant+ on the Orbitrap MS data for reprocessing of the Mayo data using the iFAMS Quant+ method. To facilitate accurate comparison of the deconvolved spectra between instrument types, the same charge state range

was used for both the Q-TOF and Orbitrap data. The most abundant six isotope peaks of both the analyte and IS were integrated for calibration with a $1/x^2$-weighted quadratic curve. Additionally, the "Segmented Baseline Correction" was applied to the integration of the Orbitrap deconvolved mass spectra which assumes baseline-resolved peaks. Since the Q-TOF deconvolved mass spectra did not have baseline resolution of isotope peaks, the "Fourier Baseline Correction" feature instead of "Segmented Baseline Correction" was applied before integration to avoid over-correction.

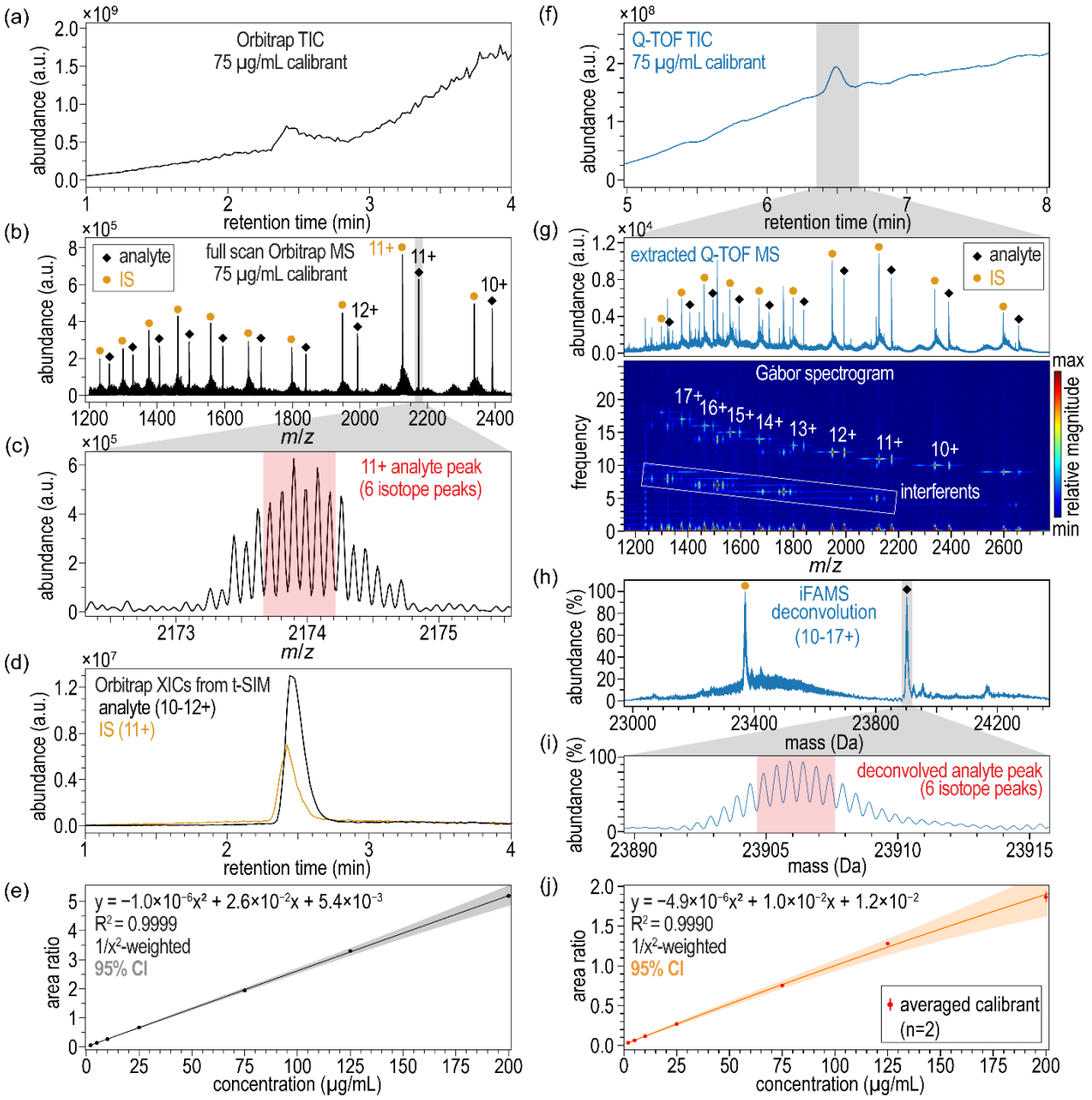

Figure 1. Mayo method and iFAMS Quant+ method workflow schematics. (a-e) Representative steps of the Mayo method workflow shown with Orbitrap data collected from one of the 75 µg/mL calibrant samples. (f-j) Representative steps of the iFAMS Quant+ method workflow shown with Q-TOF data collected from the same 75 µg/mL calibrant sample. (a) Total ion chromatogram (TIC) of the 75 µg/mL calibrant analyzed on the Orbitrap mass spectrometer. Full retention time range was considered for generating the extracted ion chromatograms (XICs). (b) Orbitrap full scan mass spectrum (MS) with vedolizumab light chain (analyte) and nivolumab light chain (IS) charge state peaks labeled with black diamonds and gold circles, respectively. (c) Full scan MS zoom-in of the analyte 11+ charge state. The top six isotope peaks (within red shaded area) were summed from the t-SIM MS for each charge state analyzed. (d) XICs were generated from integrating the t-SIM MS abundance from charge states 10+, 11+, and 12+ for

the analyte (black) and charge state 11+ for the IS (gold). XIC peaks were integrated with possible manual baseline correction for final quantitation. (e) Calibration curve from XIC peak area ratios spanning seven levels from 2 to 200 µg/mL vedolizumab. Calibration data was fit to a $1/x^2$-weighted quadratic curve, and the 95% confidence interval (CI) is shown as the gray shaded area. (f) TIC of the 75 µg/mL calibrant analyzed on the Q-TOF mass spectrometer. The MS was extracted over a 0.3 min retention time window. Note that the retention times for the Orbitrap TICs differ from the Q-TOF TICs due to LC-multiplexing on the Orbitrap setup while the Q-TOF setup ran a single channel LC. (g) Q-TOF MS with analyte and IS charge state peaks labeled with black diamonds and gold circles, respectively, and corresponding Gábor transform shown in the spectrogram below the MS. Fundamentals of the analyte and IS signal in the spectrogram were labeled with their charge state assignments. Lower-charge state interferents (indicated in the spectrogram) were easily excluded from the deconvolution. (h) iFAMS deconvolution from charge states 10-17+ of both analyte and IS. (i) Deconvolution zoom-in of the analyte peak. The top six isotope peaks (within red shaded area) were integrated for both the analyte and IS for final quantitation. (j) Calibration curve from deconvolution peak area ratios spanning seven levels from 2 to 200 µg/mL vedolizumab. Calibration data was averaged between before and after subject sample measurements then fit to a $1/x^2$-weighted quadratic curve, and the 95% CI is shown as the orange shaded area. Error bars indicate the spread in the two measurements.

Statistical evaluation. Commonly used when comparing results of two clinical tests, Passing-Bablok regression is robust and tolerant of outliers and allows for imprecision in both measurements. In typical cases, when considering the regression equation and the 95% confidence interval, one can assume the deviation between two methods is not significant if the intercept includes zero and the slope includes one. The Pearson correlation coefficient (r) is also used to describe the quality and linearity of a regression, with values larger than 0.99 typically being interpreted as indicating excellent correlation.[43] The Passing-Bablok regression algorithm in Analyse-it (Leeds, UK), with slope and intercept standard deviations estimated by the bootstrap method, was used to compare quantitation results between the Mayo method and the iFAMS Quant+ method.

Results and Discussion

Many aspects of the two methods used in this study were kept as similar as possible, however there are several noteworthy differences. The key differences included a freeze-ship-thaw step for the samples analyzed at University of Oregon, the LC/HRMS instrumentation, and the data processing and analysis methods. Since the main goals of this study were to compare the performance of the two data analysis methods, we performed a set of experiments to isolate each of these differences and assess their contributions to the final inter-laboratory quantitation results.

Freezing step experiment. Although the same five trays of processed samples were injected on both methods, the samples measured at University of Oregon required a freezing step to ensure safe shipping from Mayo Clinic. As a positive control for effects of sample freezing, two calibration sets with subject samples were analyzed at Mayo Clinic, frozen, thawed, and reanalyzed at Mayo Clinic. Although the Passing-Bablok regression for the pre- and post-freezing samples showed no significant deviation from unity ($y = -0.2636 + 1.065x$, $r = 0.763$, $n = 142$), the Pearson's r for the combined data was somewhat low (see Figure S1a). Analyzing the two data sets individually resulted in increased Pearson's r coefficients and opposing biases ($y = -0.6565 + 0.8823x$, $r = 0.836$, $n = 69$; and $y = -2.082 + 1.568x$, $r = 0.935$, $n = 73$). The 95% confidence intervals included the origin for the y-intercept of both regressions, but neither confidence interval for the regression slope included a slope of one (see Figure S1b-c). These results suggest that the freeze-thaw step can introduce a significant bias that can drift from tray to tray, but there was no alternative method available to ship the samples without the danger of them degrading or introducing contamination throughout the sample set. Since the combined data regression included the line of unity, it was concluded that freezing the samples for shipping

was tolerable, and the above Passing-Bablok regression results were used to assess whether the further results were within the magnitude of the drifting bias introduced by freezing.

Quantitative analysis comparison with identical data. In addition to the LC/MS data for the inter-laboratory comparison being acquired by laboratories some 1500 mi (2400 km) apart, they were also acquired using different LC setups and HRMS instrument types. As many LC parameters as possible, including solvents, gradients, flow rates, temperatures, and columns were kept identical, but the Mayo Clinic LC setup used three-channel multiplexing which was not available at University of Oregon. To account for longer experiment times (~3×) at University of Oregon due to running a single LC channel, calibrators were run before and after subject sample experiments, and calibration was performed by fitting the average response between the two runs of the calibrators.

While HRMS instruments were used at both labs, an Agilent 6545XT AdvanceBio Q-TOF mass spectrometer was used at University of Oregon, whereas a Thermo Scientific Q Exactive Plus Orbitrap mass spectrometer was used at Mayo Clinic. Both HRMS instruments were able to achieve isotope resolution on the t-mAb light chain subunits to varying degrees. The Orbitrap mass spectra had nearly baseline-resolved isotope peaks, while the Q-TOF mass spectra had resolution ~65% of that of the Orbitrap data based on the isotope peak widths for the vedolizumab light chain.

Although many data analysis parameters were kept as similar as possible, such as integrating the six most abundant isotope peaks for each analyte, different approaches were used to treat mass spectral signal spread across multiple charge states. The Mayo method determines background from XICs generated from a representative subset of charge states and then integrates the XIC peak for quantitative analysis. Which charge states are used depends on the

analyte and the experimental conditions. They are selected during method development based on numerous factors, with reducing interferences and maximizing specificity of the measurement being a primary consideration. Yielding adequate sensitivity by selecting charge states with sufficient relative abundance is also imperative. Minimizing the implications of charge state drift is also important when selecting charge states, determining mobile phase solvents, and optimizing source conditions. In contrast, the iFAMS Quant+ method generally uses as many charge states as possible for the deconvolution with the primary goal of maximizing the signal-to-noise ratio of the deconvolved peaks.

Another notable difference between the two methods that arises from the different strategies is that the order in which the chromatograms and mass spectra are integrated is reversed. That is, in the Mayo method, the mass spectrum is processed first to generate the XIC, which is used to determine the background and integrated for quantitation. In the iFAMS Quant+ method, the total ion chromatogram is integrated first to extract the mass spectrum, which is then deconvolved and background-subtracted before being integrated for quantitation. In principle, this change in order can have a significant impact on the baseline correction of the final integration used in the quantitation. It is not immediately obvious which strategy, if either, should result in more accurate quantitation, as some studies have shown comparable results using XIC and deconvolution approaches.[17] Emphatically, a GT-based approach to protein quantitation has never been evaluated against a previously validated protocol.

To assess the effect of the iFAMS Quant+ workflow independently on quantitation, both data analysis methods were first applied to the same LC/HRMS calibration data collected at Mayo Clinic. Five sets of calibration data were used, each with seven concentration levels spanning 2-200 µg/mL and two sets of quality control (QC) samples at four different

concentrations. Different combinations of iFAMS processing parameters were tested including charge states used for the deconvolved mass spectra (10-12+ and 10-17+). Charge states 10-17+ were selected for inclusion in all iFAMS Quant+ analyses included in this study based on QC precision and QC calculated concentrations being most consistent with the Mayo method results. Results from both methods were compared by plotting the calculated QC concentrations from iFAMS Quant+ against the calculated concentrations from the Mayo Clinic method and fit with a Passing-Bablok regression (see Figure 2). The resulting regression demonstrated excellent agreement between the two methods with the 95% confidence interval overlapping the line of unity and a good Pearson's r coefficient ($y = -0.3387 + 1.015x$, $r = 0.994$, $n = 40$). Precision was also assessed across the ten samples at each QC level and compared between the two methods (see Table 1). There was excellent agreement in precision with some small differences in % CV for the lower concentration QC levels. However, two-tailed F-tests indicate the standard deviations at every level did not differ significantly between the two methods. The most significant difference was observed at the QC II level (nominally 17.4 µg/mL vedolizumab) with a p-value = .10. These data supported that the differences in the data analysis (i.e., XIC-based vs. GT-based) methods did not significantly impact the results of the quantitation.

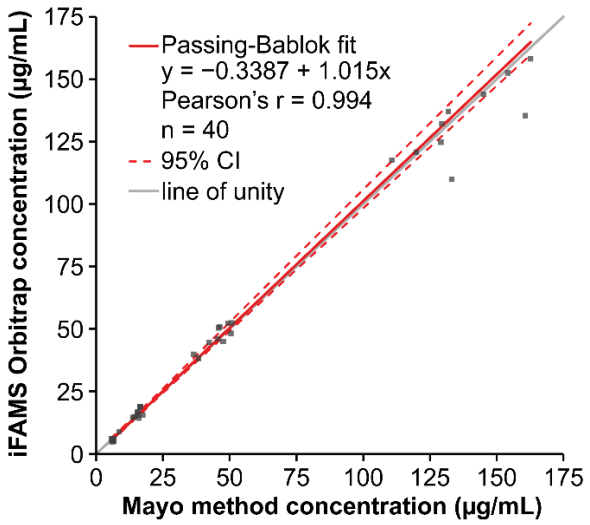

Figure 2. Quantitation method comparison QC plot on identical Orbitrap data. Concentrations were calculated for 40 QC samples (gray squares) measured with the Orbitrap MS and processed with iFAMS Quant+ and the Mayo method. The results were fit using a Passing-Bablok regression (solid red line), and the 95% confidence interval is indicated by dashed red lines. The bootstrapped 95% CI for the intercept spans −1.018 to 0.5813. The bootstrapped 95% CI for the slope spans 0.9826 to 1.065. The line of unity (y = x) is shown as the gray dashed line.

Table 1. Comparison of QC precision from replicate measurements from same analysis with different quantitation.

		QC I 6.8 µg/mL [4.5-8.3]	**QC II** 17.4 µg/mL [11.1-20.5]	**QC III** 48 µg/mL [36-68]	**QC IV** 146 µg/mL [105-195]
Mayo method	Mean (µg/mL)	6.5	15.7	45	138
	% CV	12%	7%	11%	13%
iFAMS method (Orbitrap data)	Mean (µg/mL)	5.9	16.4	47	133
	% CV	19%	11%	11%	12%
Two-tailed F-test P-value		.283	.097	.944	.708

Inter-laboratory quantitation comparison. After being analyzed at Mayo Clinic, the same five sets of samples described above were also frozen, shipped, thawed, and analyzed at

University of Oregon on an LC/Q-TOF. For each tray, the average response for each calibrant was used to quantitate sets of 79 subject samples with QC samples placed at the front and back of each sample set. The iFAMS Quant+ quantitation results of the Q-TOF data were then compared to the results from the Mayo method. The QC comparison and precision results were highly consistent with the results from the comparison across identical data. The QC comparison Passing-Bablok regression for these data acquired with different instruments (see Figure 3) resulted in a slope and intercept slightly closer to unity and a larger Pearson's r coefficient ($y = 0.2609 + 1.007x$, $r = 0.996$, $n = 40$) than for the above-described regression of iFAMS Quant+ results vs. Mayo method results on the same (Orbitrap) instrument. Precision analysis revealed slightly improved % CVs for the two lower concentration QC levels, and, again, no significant differences in standard deviations between the two methods and larger associated p-values for all but the lowest QC level (see Table 2). The QC I (nominal 6.5 µg/mL vedolizumab) p-value decreased from .28 (same instrument) to .17 (different instruments), but the new p-value still indicated low significance to the differences in precision between the two methods.

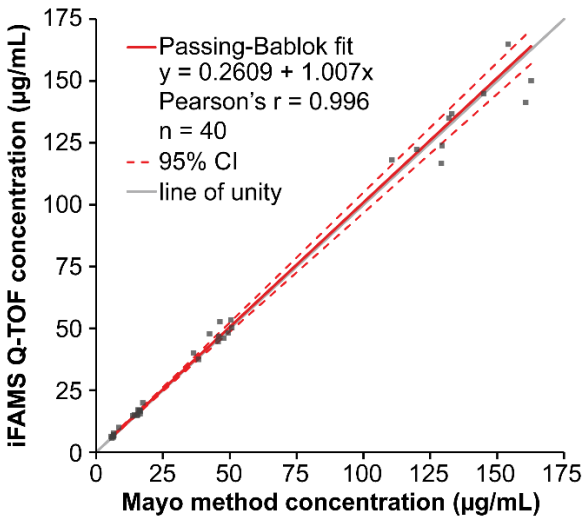

Figure 3. Quantitation method comparison QC plot on inter-laboratory data. Concentrations were calculated for 40 QC samples (gray squares) measured with the Orbitrap MS for the Mayo method concentrations and the Q-TOF MS for the iFAMS Quant+ method concentrations. The results were fit using a Passing-Bablok regression (solid red line), and the 95% confidence interval (CI) is indicated by the dashed red lines. The bootstrapped 95% CI for the intercept spans −0.3152 to 0.9515. The bootstrapped 95% CI for the slope spans 0.9612 to 1.051. The line of unity (y = x) is shown as the gray dashed line.

Table 2. Comparison of QC precision from inter-laboratory replicate measurements.

		QC I 6.8 µg/mL [4.5-8.3]	**QC II** 17.4 µg/mL [11.1-20.5]	**QC III** 48 µg/mL [36-68]	**QC IV** 146 µg/mL [105-195]
Mayo method	Mean (µg/mL)	6.5	15.7	45	138
	% CV	12%	7%	11%	13%
iFAMS method (Q-TOF data)	Mean (µg/mL)	6.8	16.2	47	135
	% CV	18%	10%	11%	12%
Two-tailed F-test P-value		.166	.578	.920	.724

The subject sample results determined using the two different instruments were compared by a Passing-Bablok regression after removing samples below the lower limit of quantitation (2 μg/mL, established for the Mayo method).[16] The regression (see Figure 4) showed good correlation with a small but significant difference, as indicated by the 95% confidence interval including the origin but not a slope of one ($y = 0.2796 + 0.9154x$, $r = 0.958$, $n = 351$). These results were compared to a previous study by Mayo Clinic on mAb light chain quantitation, in which intact light chain LC/HRMS quantitation was compared to two peptide LC-MS/MS assays and two commercially available ELISAs. The first peptide LC-MS/MS method was developed at Mayo Clinic using an AB Sciex API 5000 Triple Quad, and the results strongly agreed with the Mayo light chain method results.[16,44] In comparison, although the iFAMS and Mayo methods described here differed according to the Passing-Bablok analysis, the magnitude of the difference was much smaller than the difference between the Mayo method and three of the four alternative assays (IDKmonitor® peptide LC-MS/MS assay and ELISA, and TDM InformTx™ ELISA) performed in the previous Mayo study.[16] Additionally, a Welch's T-test was used to compare the slope of the Passing-Bablok regression to that from the combined freezing experiment data. The results of this statistical test indicated that the observed difference in slopes was within range of the drifting bias associated with sample freezing (see above) with a p-value of .22. Therefore, the freezing step could not be ruled out as a major contributing source for the observed differences between the inter-laboratory results determined using the two quantitation methods on different instruments.

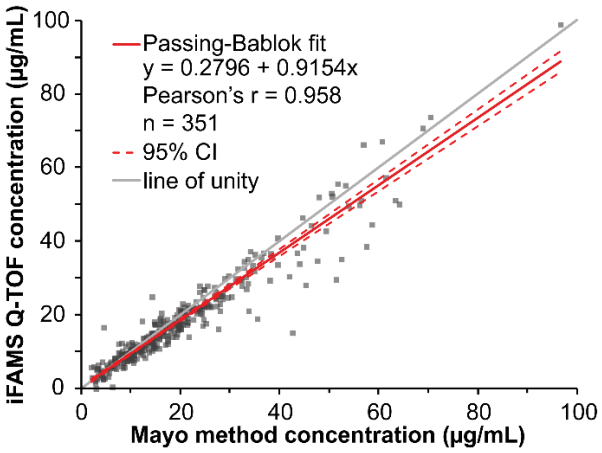

Figure 4. Inter-laboratory subject sample method comparison. Concentrations calculated for 351 subject samples (gray squares) measured with the Orbitrap MS for the Mayo method concentrations and the Q-TOF MS for the iFAMS Quant+ method concentrations were fit using a Passing-Bablok regression (solid red line). The bounds of the 95% confidence interval (CI) are shown with the red dashed lines. The bootstrapped 95% CI for the intercept spans −0.2526 to 0.7673. The bootstrapped 95% CI for the slope spans 0.8825 to 0.9495. The line of unity (y = x) is shown as the solid gray line.

Outlier deconvolution analysis. Excellent agreement between the iFAMS Quant+ and Mayo methods was observed for most of the subject samples with 74% of the 351 samples having less than 20% difference. To investigate sources of discrepancies for the other subject samples (i.e., with ≥20% difference), a subset of sixteen samples was selected to have mass spectra extracted from each major XIC peak and screened based on accurate mass of each contributing charge state before and after deconvolution. To serve as a basis for comparison, a subject sample with 15% difference in concentration was also investigated (see Figure S2). This control sample's XIC had a well resolved and isolated analyte peak, and good isotope resolution with high mass accuracy was observed in the iFAMS deconvolved mass spectrum. Examination of the individually deconvolved isotope distribution for each selected charge state, a capability unique to iFAMS deconvolution software, further indicated that the total deconvolved isotope distribution was well supported by all charge states in the raw mass spectrum.

Of the screened samples with >20% difference between the University of Oregon and Mayo Clinic results, two major types of discrepancies were observed: a clear drop in analyte signal in the Q-TOF data as compared to the Orbitrap data regardless of analysis method (XIC vs. iFAMS Quant+) used, and analyte signal interference at similar *m*/*z* of several or all observed analyte charge states. For the samples that exhibited a drop in analyte signal, the Mayo and iFAMS methods agreed on concentration within tolerance when determined from the Orbitrap data, but the concentrations determined from the Q-TOF data were as much as 35-65% lower (see Figure 5). The analyte and internal standard peaks in the raw and deconvolved mass spectra showed no signs of interfering signal for either instrument. XICs were generated from the Q-TOF mass spectrum to assess whether the loss of signal could be attributed to the elution peak shifting outside of the fixed retention time window. Figure S3 in the Supporting Information shows the Q-TOF XICs from the same sample as shown in Figure 5. The retention time window was well centered about the analyte and IS elution peaks, but an additional small peak outside the retention time window was present in the analyte XIC that did not occur in the Orbitrap analyte XIC. The sample was processed again from the mass spectrum extracted over a wider retention time that included both analyte peaks, but the resulting concentration (26.6 µg/mL) did not increase enough from the previously calculated concentration (26.0 µg/mL) to account for the loss of signal between instruments. Thus, the loss in analyte signal for these samples analyzed with the Q-TOF instrument was attributed to analyte degradation or aggregation from the freeze-ship-thaw step, though this analysis does not rule out other possible contributing causes, such as contamination of these samples with proteases or other chemical effects. Differences in chromatographic performance or ion suppression/enhancement for the two mass spectrometers is also a possible explanation of these observations.

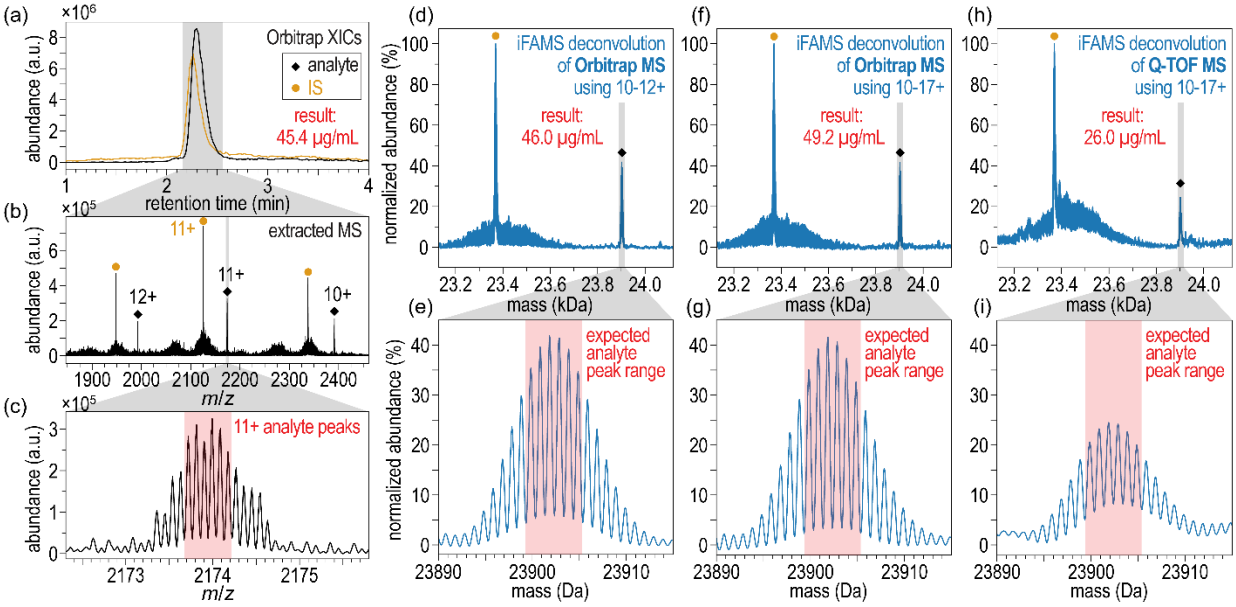

Figure 5. Outlier example of drop in analyte signal in the Q-TOF mass spectrum. (a) Extracted ion chromatograms (XICs) generated from the Orbitrap mass spectrum (MS). The analyte XIC (black) was generated from charge states 10-12+, and the IS XIC (gold) was generated from charge state 11+. (b) Extracted full scan MS from a 2.16-2.49 min retention time window zoomed in on the 10-12+ charge states. (c) MS zoom-in on analyte 11+ charge state with top six isotope peaks highlighted in red. (d) iFAMS deconvolution using charge states 10-12+ from the Orbitrap MS with analyte (black diamond) and IS peaks (gold circle) labeled. (e) Zoom-in on the analyte peak from the deconvolution in (d) with the top six isotope peaks highlighted in red. (f) iFAMS deconvolution using charge states 10-17+ from the Orbitrap MS with analyte (black diamond) and IS peaks (gold circle) labeled. (g) Zoom-in on the analyte peak from the deconvolution in (f) with the top six isotope peaks highlighted in red. (h) iFAMS deconvolution using charge states 10-17+ from the Q-TOF MS extracted from a 6.15-6.45 min retention time window with analyte (black diamond) and IS peaks (gold circle) labeled. (i) Zoom-in on the analyte peak from the deconvolution in (h) with the top six isotope peaks highlighted in red.

Most of the selected samples with >20% difference between the two methods exhibited interferent signal in both the XIC and the iFAMS Quant+ deconvolved mass spectrum. In an extreme case (see Figure 6), the interfering signal had nearly the same retention time as the analyte and was only resolved by combining multiple charge states. This made the interferent exceptionally challenging to detect in the XIC and the raw mass spectrum. However, use of iFAMS Quant+ to combine charge states for the deconvolved mass spectrum, revealed an interferent peak centroid at 3-4 Da light of the expected analyte peak centroid. This interferent

was visible from charge states 10-12+ but was more evident when utilizing more charges states, and it was visible in both deconvolved mass spectra from the Orbitrap and Q-TOF data. Although the analyte peaks appear to be more prominent than the interferent peaks in the deconvolved mass spectrum from charge states 10-12+ (Figure 6e), the most abundant isotope peak observed is 2 Da heavier than expected (~80 ppm). Figure S4 in the Supporting Information shows the contribution of each charge state to the combined deconvolved mass spectrum. These results demonstrate a clear advantage of using a GT-based approach in a protein quantitation protocol that combines mass spectral data from multiple charge states. That is, with the increase in the signal-to-noise ratio that comes from combining several charge states, it was possible to detect a change in the isotope distribution near the expected analyte mass that was not obvious in the XIC. Although the interferent had to be detected manually, automatic screening of the average mass centroid could be used to warn users of potential interferents in future versions of iFAMS Quant+, and future versions of this software will include automatic flagging of possible interferents overlapped with the analyte of interest.

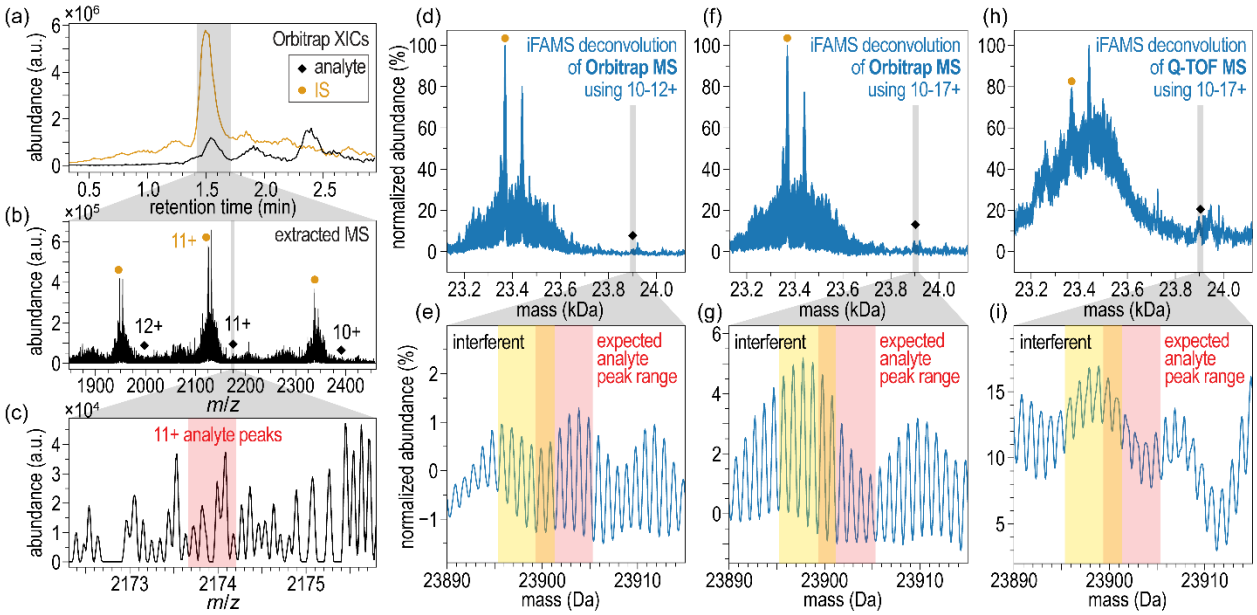

Figure 6. Outlier example of analyte signal interference. (a) Extracted ion chromatograms (XICs) generated from the Orbitrap mass spectrum (MS). The analyte XIC (black) was generated from charge states 10-12+, and the IS XIC (gold) was generated from charge state 11+. (b) Extracted MS from a 1.41-1.71 min retention time window zoomed in on the 10-12+ charge states. (c) MS zoom-in on analyte 11+ charge state with the expected range of the top six isotope peaks highlighted in red. (d) iFAMS deconvolution using charge states 10-12+ from the Orbitrap MS with analyte (black diamond) and IS peaks (gold circle) labeled. (e) Zoom-in on the analyte peak from the deconvolution in (d) with the expected range of the top six isotope peaks highlighted in red and an observed interferent based on average mass deviation highlighted in yellow. (f) iFAMS deconvolution using charge states 10-17+ from the Orbitrap MS with analyte (black diamond) and IS peaks (gold circle) labeled. (g) Zoom-in on the analyte peak from the deconvolution in (f) with the expected range of the top six isotope peaks highlighted in red and an observed interferent based on average mass deviation highlighted in yellow. (h) iFAMS deconvolution using charge states 10-17+ from the Q-TOF MS with analyte (black diamond) and IS peaks (gold circle) labeled. (i) Zoom-in on the analyte peak from the deconvolution in (h) with the expected range of the top six isotope peaks highlighted in red and an observed interferent based on average mass deviation highlighted in yellow.

Conclusions

This study demonstrates the efficacy, reproducibility, and advantages of using Gábor Transform-based deconvolution, as implemented in iFAMS Quant+, for t-mAb quantitation and compares its performance against a validated method from Mayo Clinic. Despite the differences in LC/HRMS instrumentation and sample handling, particularly the freezing step necessary for

inter-laboratory sample transport, iFAMS Quant+ showed strong agreement with the Mayo method in both QC and subject sample quantitation. This comparison using real clinical samples highlights its potential for broader applications, especially for LC/MS techniques for quantitation of large molecules, through middle-up and top-down proteomics more broadly or other omics fields. Although a slight bias was observed between the quantitative analyses for samples analyzed between the two laboratories, the magnitude of the difference was within the observed bias seen due to freezing of the samples, and the overall performance of iFAMS Quant+ remained highly reliable. Further potential effects of the freeze-ship-thaw step found in this study included apparent loss of analyte for a small number of samples and serve as a caveat for inter-laboratory quantitation studies by LC/MS.

This study also illustrates unique advantages of deconvolution with iFAMS Quant+ to understand discrepancies between results from the two methods, as for the subject sample for which deconvolution with iFAMS Quant+ revealed an interferent 3-4 Da lighter than the 24 kDa analyte. Future improvements to iFAMS Quant and iFAMS Quant+ will feature automated detection and flagging of such potential interferents by comparing shape and centroid of the deconvolved experimental isotope distribution to that expected for the analyte of interest. iFAMS Quant Python-coded open-source software is publicly available at https://github.com/prellgroup/iFAMS/releases, and an executable file for iFAMS Quant+ (which can directly interact with and batch process Agilent .d files) can be licensed from the University of Oregon by contacting the authors.

Supporting Information

The Supporting Information is available free of charge at: https://pubs.acs.org

- Detailed instrument acquisition parameters; regression results from the freezing step experiment; example of good method agreement for a subject sample; additional figures for the example of drop in signal between instruments; and additional figures for the example of analyte interferent.

Acknowledgments

Research reported in this publication was supported by the National Science Foundation (award CHE-1752994 to JSP) and Agilent Technologies, Inc. (University Relations award #4524). The content is solely the responsibility of the authors and does not necessarily represent the official views of the National Science Foundation.

Conflict of Interest Disclosure

The Agilent 6545XT AdvanceBio Q-TOF mass spectrometer with a 1290 Infinity II LC used for this research was generously loaned to University of Oregon by Agilent Technologies, Inc. This research was supported in part by a University Relations from Agilent Technologies, Inc., award to JSP (#4524).

TOC Graphic

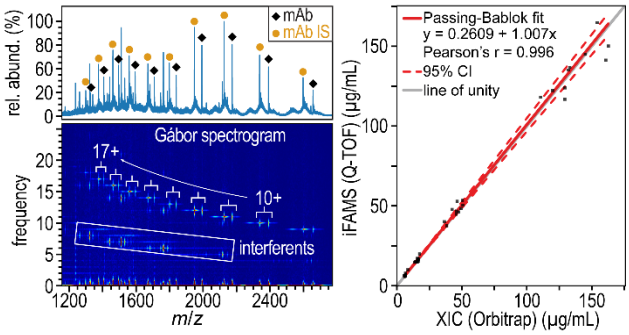
rel. abund. (%)
mAb
mAb IS
Gábor spectrogram
17+
10+
interferents
frequency
m/z
Passing-Bablok fit
y = 0.2609 + 1.007x
Pearson's r = 0.996
95% CI
line of unity
iFAMS (Q-TOF) (µg/mL)
XIC (Orbitrap) (µg/mL)

References

(1) Maloney, D. G.; Grillo-López, A. J.; White, C. A.; Bodkin, D.; Schilder, R. J.; Neidhart, J. A.; Janakiraman, N.; Foon, K. A.; Liles, T.-M.; Dallaire, B. K.; Wey, K.; Royston, I.; Davis, T.; Levy, R. IDEC-C2B8 (Rituximab) Anti-CD20 Monoclonal Antibody Therapy in Patients With Relapsed Low-Grade Non-Hodgkin's Lymphoma. *Blood* **1997**, *90* (6), 2188–2195. https://doi.org/10.1182/blood.V90.6.2188.

(2) Radner, H.; Aletaha, D. Anti-TNF in Rheumatoid Arthritis: An Overview. *Wien. Med. Wochenschr.* **2015**, *165* (1), 3–9. https://doi.org/10.1007/s10354-015-0344-y.

(3) Zahavi, D.; Weiner, L. Monoclonal Antibodies in Cancer Therapy. *Antibodies* **2020**, *9* (3), 34. https://doi.org/10.3390/antib9030034.

(4) Hwang, K.; Yoon, J. H.; Lee, J. H.; Lee, S. Recent Advances in Monoclonal Antibody Therapy for Colorectal Cancers. *Biomedicines* **2021**, *9* (1), 39. https://doi.org/10.3390/biomedicines9010039.

(5) Lim, S. H.; Kim, K.; Choi, C.-I. Pharmacogenomics of Monoclonal Antibodies for the Treatment of Rheumatoid Arthritis. *J. Pers. Med.* **2022**, *12* (8), 1265. https://doi.org/10.3390/jpm12081265.

(6) Briani, C.; Visentin, A. Therapeutic Monoclonal Antibody Therapies in Chronic Autoimmune Demyelinating Neuropathies. *Neurotherapeutics* **2022**, *19* (3), 874–884. https://doi.org/10.1007/s13311-022-01222-x.

(7) Silva-Ferreira, F.; Afonso, J.; Pinto-Lopes, P.; Magro, F. A Systematic Review on Infliximab and Adalimumab Drug Monitoring: Levels, Clinical Outcomes and Assays. *Inflamm. Bowel Dis.* **2016**, *22* (9), 2289–2301. https://doi.org/10.1097/MIB.0000000000000855.

(8) Temrikar, Z. H.; Suryawanshi, S.; Meibohm, B. Pharmacokinetics and Clinical Pharmacology of Monoclonal Antibodies in Pediatric Patients. *Pediatr. Drugs* **2020**, *22* (2), 199–216. https://doi.org/10.1007/s40272-020-00382-7.

(9) Paci, A.; Desnoyer, A.; Delahousse, J.; Blondel, L.; Maritaz, C.; Chaput, N.; Mir, O.; Broutin, S. Pharmacokinetic/Pharmacodynamic Relationship of Therapeutic Monoclonal Antibodies Used in Oncology: Part 1, Monoclonal Antibodies, Antibody-Drug Conjugates and Bispecific T-Cell Engagers. *Eur. J. Cancer* **2020**, *128*, 107–118. https://doi.org/10.1016/j.ejca.2020.01.005.

(10) Vande Casteele, N.; Buurman, D. J.; Sturkenboom, M. G. G.; Kleibeuker, J. H.; Vermeire, S.; Rispens, T.; van der Kleij, D.; Gils, A.; Dijkstra, G. Detection of Infliximab Levels and Anti-Infliximab Antibodies: A Comparison of Three Different Assays. *Aliment. Pharmacol. Ther.* **2012**, *36* (8), 765–771. https://doi.org/10.1111/apt.12030.

(11) Lázár-Molnár, E.; Delgado, J. C. Immunogenicity Assessment of Tumor Necrosis Factor Antagonists in the Clinical Laboratory. *Clin. Chem.* **2016**, *62* (9), 1186–1198. https://doi.org/10.1373/clinchem.2015.242875.

(12) Hart, M. H.; de Vrieze, H.; Wouters, D.; Wolbink, G.-J.; Killestein, J.; de Groot, E. R.; Aarden, L. A.; Rispens, T. Differential Effect of Drug Interference in Immunogenicity

Assays. *J. Immunol. Methods* **2011**, *372* (1), 196–203. https://doi.org/10.1016/j.jim.2011.07.019.

(13) Barnidge, D. R.; Dasari, S.; Botz, C. M.; Murray, D. H.; Snyder, M. R.; Katzmann, J. A.; Dispenzieri, A.; Murray, D. L. Using Mass Spectrometry to Monitor Monoclonal Immunoglobulins in Patients with a Monoclonal Gammopathy. *J. Proteome Res.* **2014**, *13* (3), 1419–1427. https://doi.org/10.1021/pr400985k.

(14) Jenkins, R.; Duggan, J. X.; Aubry, A.-F.; Zeng, J.; Lee, J. W.; Cojocaru, L.; Dufield, D.; Garofolo, F.; Kaur, S.; Schultz, G. A.; Xu, K.; Yang, Z.; Yu, J.; Zhang, Y. J.; Vazvaei, F. Recommendations for Validation of LC-MS/MS Bioanalytical Methods for Protein Biotherapeutics. *AAPS J.* **2014**, *17* (1), 1–16. https://doi.org/10.1208/s12248-014-9685-5.

(15) Ladwig, P. M.; Barnidge, D. R.; Willrich, M. A. V. Mass Spectrometry Approaches for Identification and Quantitation of Therapeutic Monoclonal Antibodies in the Clinical Laboratory. *Clin. Vaccine Immunol.* **2017**, *24* (5), e00545-16. https://doi.org/10.1128/CVI.00545-16.

(16) Cradic, K. W.; Ladwig, P. M.; Rivard, A. L.; Katrangi, W.; Wintgens, K. F.; Willrich, M. A. V. Vedolizumab Quantitation Using High-Resolution Accurate Mass-Mass Spectrometry Middle-up Protein Subunit: Method Validation. *Clin. Chem. Lab. Med. CCLM* **2020**, *58* (6), 864–872. https://doi.org/10.1515/cclm-2019-0862.

(17) Qiu, X.; Kang, L.; Case, M.; Weng, N.; Jian, W. Quantitation of Intact Monoclonal Antibody in Biological Samples: Comparison of Different Data Processing Strategies. *Bioanalysis* **2018**, *10* (13), 1055–1067. https://doi.org/10.4155/bio-2018-0016.

(18) Qiu, X.; Hale, W. A.; Wong, D. Ultra-Sensitive Intact Monoclonal Antibody Quantification Using AssayMAP Bravo Liquid Handling Platform and 6545XT AdvanceBio LC/Q-TOF Mass Spectrometer. *Agilent Technologies application note* **2020**. https://doi.org/publication number 5994-1984EN.

(19) Jian, W.; Kang, L.; Burton, L.; Weng, N. A Workflow for Absolute Quantitation of Large Therapeutic Proteins in Biological Samples at Intact Level Using LC-HRMS. *Bioanalysis* **2016**, *8* (16), 1679–1691. https://doi.org/10.4155/bio-2016-0096.

(20) Dhenin, J.; Lafont, V.; Dupré, M.; Krick, A.; Mauriac, C.; Chamot-Rooke, J. Monitoring mAb Proteoforms in Mouse Plasma Using an Automated Immunocapture Combined with Top-down and Middle-down Mass Spectrometry. *PROTEOMICS* **2024**, *24* (3–4), 2300069. https://doi.org/10.1002/pmic.202300069.

(21) Fornelli, L.; Srzentić, K.; Huguet, R.; Mullen, C.; Sharma, S.; Zabrouskov, V.; Fellers, R. T.; Durbin, K. R.; Compton, P. D.; Kelleher, N. L. Accurate Sequence Analysis of a Monoclonal Antibody by Top-Down and Middle-Down Orbitrap Mass Spectrometry Applying Multiple Ion Activation Techniques. *Anal. Chem.* **2018**, *90* (14), 8421–8429. https://doi.org/10.1021/acs.analchem.8b00984.

(22) Kellie, J. F.; Kehler, J. R.; Karlinsey, M. Z.; Summerfield, S. G. Toward Best Practices in Data Processing and Analysis for Intact Biotherapeutics by MS in Quantitative Bioanalysis. *Bioanalysis* **2017**, *9* (23), 1883–1893. https://doi.org/10.4155/bio-2017-0179.

(23) Todoroki, K.; Mizuno, H.; Sugiyama, E.; Toyo'oka, T. Bioanalytical Methods for Therapeutic Monoclonal Antibodies and Antibody–Drug Conjugates: A Review of Recent

Advances and Future Perspectives. *J. Pharm. Biomed. Anal.* **2020**, *179*, 112991. https://doi.org/10.1016/j.jpba.2019.112991.

(24) Rolland, A. D.; Prell, J. S. Approaches to Heterogeneity in Native Mass Spectrometry. *Chem. Rev.* **2022**, *122* (8), 7909–7951. https://doi.org/10.1021/acs.chemrev.1c00696.

(25) Kafader, J. O.; Melani, R. D.; Schachner, L. F.; Ives, A. N.; Patrie, S. M.; Kelleher, N. L.; Compton, P. D. Native vs Denatured: An in Depth Investigation of Charge State and Isotope Distributions. *J. Am. Soc. Mass Spectrom.* **2020**, *31* (3), 574–581. https://doi.org/10.1021/jasms.9b00040.

(26) Shepherd, S. O.; Green, A. W.; Resendiz, E. S.; Newton, K. R.; Kurulugama, R. T.; Prell, J. S. Effects of Nano-Electrospray Ionization Emitter Position on Unintentional In-Source Activation of Peptide and Protein Ions. *J. Am. Soc. Mass Spectrom.* **2024**, *35* (3), 498–507. https://doi.org/10.1021/jasms.3c00371.

(27) Alelyunas, Y. W.; Shion, H.; Edwards, I.; Wrona, M. Intact Trastuzumab Monoclonal Antibody Quantification Using the Xevo G2-XS QTof High Resolution Mass Spectrometer. *Waters application note* **2018**. https://doi.org/publication number 720006222EN.

(28) Zhang, L.; Vasicek, L. A.; Hsieh, S.; Zhang, S.; Bateman, K. P.; Henion, J. Top-down LC–MS Quantitation of Intact Denatured and Native Monoclonal Antibodies in Biological Samples. *Bioanalysis* **2018**, *10* (13), 1039–1054. https://doi.org/10.4155/bio-2017-0282.

(29) Kellie, J. F.; Schneck, N. A.; Causon, J. C.; Baba, T.; Mehl, J. T.; Pohl, K. I. Top-Down Characterization and Intact Mass Quantitation of a Monoclonal Antibody Drug from Serum by Use of a Quadrupole TOF MS System Equipped with Electron-Activated Dissociation. *J. Am. Soc. Mass Spectrom.* **2023**, *34* (1), 17–26. https://doi.org/10.1021/jasms.2c00206.

(30) Reinhold, B. B.; Reinhold, V. N. Electrospray Ionization Mass Spectrometry: Deconvolution by an Entropy-Based Algorithm. *J. Am. Soc. Mass Spectrom.* **1992**, *3* (3), 207–215. https://doi.org/10.1016/1044-0305(92)87004-I.

(31) Bern, M.; Caval, T.; Kil, Y. J.; Tang, W.; Becker, C.; Carlson, E.; Kletter, D.; Sen, K. I.; Galy, N.; Hagemans, D.; Franc, V.; Heck, A. J. R. Parsimonious Charge Deconvolution for Native Mass Spectrometry. *J. Proteome Res.* **2018**, *17* (3), 1216–1226. https://doi.org/10.1021/acs.jproteome.7b00839.

(32) Marty, M. T.; Baldwin, A. J.; Marklund, E. G.; Hochberg, G. K. A.; Benesch, J. L. P.; Robinson, C. V. Bayesian Deconvolution of Mass and Ion Mobility Spectra: From Binary Interactions to Polydisperse Ensembles. *Anal. Chem.* **2015**, *87* (8), 4370–4376. https://doi.org/10.1021/acs.analchem.5b00140.

(33) Horn, D. M.; Zubarev, R. A.; McLafferty, F. W. Automated Reduction and Interpretation of High Resolution Electrospray Mass Spectra of Large Molecules. *J. Am. Soc. Mass Spectrom.* **2000**, *11* (4), 320–332. https://doi.org/10.1016/S1044-0305(99)00157-9.

(34) Cleary, S. P.; Li, H.; Bagal, D.; Loo, J. A.; Campuzano, I. D. G.; Prell, J. S. Extracting Charge and Mass Information from Highly Congested Mass Spectra Using Fourier-Domain Harmonics. *J. Am. Soc. Mass Spectrom.* **2018**, *29* (10), 2067–2080. https://doi.org/10.1007/s13361-018-2018-7.

(35) Bults, P.; Sonesson, A.; Knutsson, M.; Bischoff, R.; van de Merbel, N. C. Intact Protein Quantification in Biological Samples by Liquid Chromatography – High-Resolution Mass Spectrometry: Somatropin in Rat Plasma. *J. Chromatogr. B* **2020**, *1144*, 122079. https://doi.org/10.1016/j.jchromb.2020.122079.

(36) Kellie, J. F.; Tran, J. C.; Jian, W.; Jones, B.; Mehl, J. T.; Ge, Y.; Henion, J.; Bateman, K. P. Intact Protein Mass Spectrometry for Therapeutic Protein Quantitation, Pharmacokinetics, and Biotransformation in Preclinical and Clinical Studies: An Industry Perspective. *J. Am. Soc. Mass Spectrom.* **2021**, *32* (8), 1886–1900. https://doi.org/10.1021/jasms.0c00270.

(37) Robey, M. T.; Utley, D.; Greer, J. B.; Fellers, R. T.; Kelleher, N. L.; Durbin, K. R. Advancing Intact Protein Quantitation with Updated Deconvolution Routines. *Anal. Chem.* **2023**, *95* (40), 14954–14962. https://doi.org/10.1021/acs.analchem.3c02345.

(38) Research, C. for D. E. and. *Bioanalytical Method Validation Guidance for Industry*. https://www.fda.gov/regulatory-information/search-fda-guidance-documents/bioanalytical-method-validation-guidance-industry (accessed 2024-02-02).

(39) Cleary, S. P.; Thompson, A. M.; Prell, J. S. Fourier Analysis Method for Analyzing Highly Congested Mass Spectra of Ion Populations with Repeated Subunits. *Anal. Chem.* **2016**, *88* (12), 6205–6213. https://doi.org/10.1021/acs.analchem.6b01088.

(40) Cleary, S. P.; Prell, J. S. Liberating Native Mass Spectrometry from Dependence on Volatile Salt Buffers by Use of Gábor Transform. *ChemPhysChem* **2019**, *20* (4), 519–523. https://doi.org/10.1002/cphc.201900022.

(41) Swansiger, A. K.; Marty, M. T.; Prell, J. S. Fourier-Transform Approach for Reconstructing Macromolecular Mass Defect Profiles. *J. Am. Soc. Mass Spectrom.* **2022**, *33* (1), 172–180. https://doi.org/10.1021/jasms.1c00317.

(42) Meldrum, K. L.; Swansiger, A. K.; Daniels, M. M.; Hale, W. A.; Kirmiz Cody, C.; Qiu, X.; Knierman, M.; Sausen, J.; Prell, J. S. Gábor Transform-Based Signal Isolation, Rapid Deconvolution, and Quantitation of Intact Protein Ions with Mass Spectrometry. *Anal. Chem.* **2024**. https://doi.org/10.1021/acs.analchem.4c00978.

(43) Bilić-Zulle, L. Comparison of Methods: Passing and Bablok Regression. *Biochem. Medica* **2011**, *21* (1), 49–52. https://doi.org/10.11613/BM.2011.010.

(44) Willrich, M. A. V.; Murray, D. L.; Barnidge, D. R.; Ladwig, P. M.; Snyder, M. R. Quantitation of Infliximab Using Clonotypic Peptides and Selective Reaction Monitoring by LC–MS/MS. *Int. Immunopharmacol.* **2015**, *28* (1), 513–520. https://doi.org/10.1016/j.intimp.2015.07.007.

Supporting Information for

Gábor Transform-Based Antibody Quantitation in Serum: An Inter-Laboratory Liquid Chromatography/High-Resolution Mass Spectrometry Investigation

Kayd L. Meldrum[1], Andrew K. Swansiger[1], Jacob Koscho[1], Lily Miller[1], John Sausen[2], Anthony D. Maus[3], Paula M. Ladwig[3], Maria A. V. Willrich[3], James S. Prell[1,4,*]

[1]Department of Chemistry and Biochemistry, 1253 University of Oregon, Eugene, OR 97403-1253, USA

[2]Agilent Technologies, Inc., 5301 Stevens Creek Blvd., Santa Clara, CA 95051, USA

[3]Department of Laboratory Medicine and Pathology, Mayo Clinic, 200 First Street SW, Rochester, MN 55905, USA

[4]Materials Science Institute, 1252 University of Oregon, Eugene, OR 97403-1252, USA

Submitted to *Analytical Chemistry*

21 August 2024

[*]Corresponding author email: jprell@uoregon.edu

Table of Contents

Table S1. Liquid chromatography (LC) acquisition parameters.

LC Parameters	
Column	2.1 × 75 mm, 5-µm Agilent Poroshell 300SB-C3 column
Autosampler Thermostat	10 °C
Solvent A	0.1% formic acid in water
Solvent B	1% formic acid in 9% 2-propanol and 90% acetonitrile
Gradient	0 to 1.5 minutes, 10% B 1.5 to 2.5 minutes, 10 to 25% B 2.5 to 10.5 minutes, 25 to 34 % B 10.5 to 11 minutes, 34 to 50 % B 11 to 11.5 minutes, 50 to 98 % B 11.5 to 13.5 minutes, 98 % B 13.5 to 14 minutes, 98 to 10 % B 14 to 17 minutes, 10 % B
Multicolumn Thermostat Temperature	60 °C
Flow Rate	0.3 mL/min
Injection Volume	10 µL

Table S2. Orbitrap mass spectrometer (MS) acquisition parameters.

Q Exactive Plus Orbitrap MS Parameters	
Source	Heated electrospray ion source (HESI)
Sheath Gas Flow Rate	50 a.u.
Aux Gas Flow Rate	12 a.u.
Sweep Gas Flow Rate	0 a.u.
Spray Voltage	3.50 kV
Capillary Temperature	300 °C
S-lens RF Level	65.0
Aux Gas Heater Temperature	300 °C
Mass Range	*m*/*z* 1200 to 2500
Automatic Gain Control Target	1e6
Maximum Injection Time	500 ms
t-SIM Mass Range	*m*/*z* 1900 to 2400
t-SIM Automatic Gain Control	2e5
t-SIM Maximum Injection Time	125 ms

Table S3. Q-TOF mass spectrometer (MS) acquisition parameters.

Agilent 6545XT AdvanceBio Q-TOF MS Parameters	
Source	Dual Agilent Jet Stream
Gas Temperature	350 °C
Gas Flow	13 L/min
Nebulizer	45 psi
Sheath Gas Temperature	380 °C
Sheath Gas Flow	12 L/min
Vcap	5500 V
Nozzle Voltage	2000 V
Fragmentor	380 V
Skimmer	140 V
Quad AMU	*m*/*z* 125.2
Mass Range	*m*/*z* 1000 to 3200
Acquisition Rate	1.0 spectra/s
Reference Mass	922.0098 Da
Acquisition Mode	Positive, high-resolution mode (4GHz)

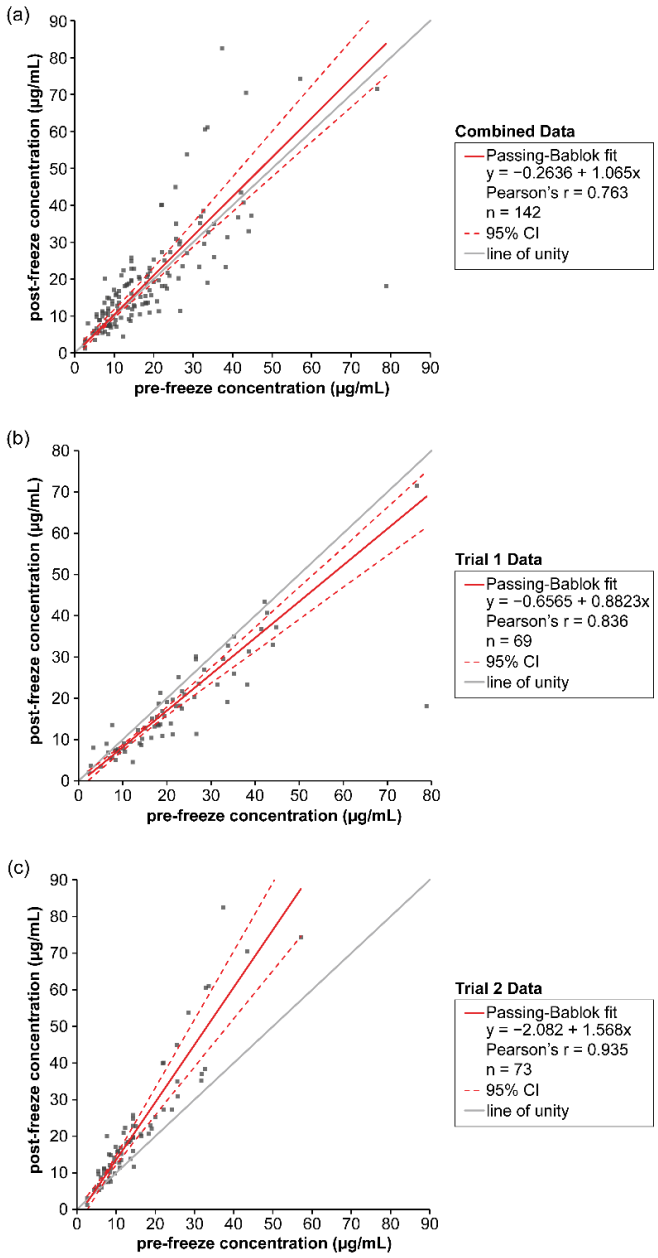

Figure S1. Freeze-thaw effect on Mayo method quantitation results. Each subfigure compares the Mayo method quantitation results of subject samples measured on the same LC-Orbitrap MS before and after freezing. The solid red line is the Passing-Bablok regression line. The dashed red lines indicate the 95% confidence interval (CI). The solid gray line (y = x) indicates the line of unity. (a) Passing-Bablok regression for the combined (n = 142) data set from two trays of samples. The bootstrapped 95% CI for the intercept spans −1.720 to 1.202. The bootstrapped 95% CI for the slope spans 0.9407 to 1.202. (b) Passing-Bablok regression for the first tray of samples (n = 69). The bootstrapped 95% CI for the intercept spans −2.089 to 0.6134. The bootstrapped 95% CI for the slope spans 0.7727 to 0.9756. (c) Passing-Bablok regression for the second tray of samples (n=73). The bootstrapped 95% CI for the intercept spans −4.972 to 0.1917. The bootstrapped 95% CI for the slope spans 1.312 to 1.867.

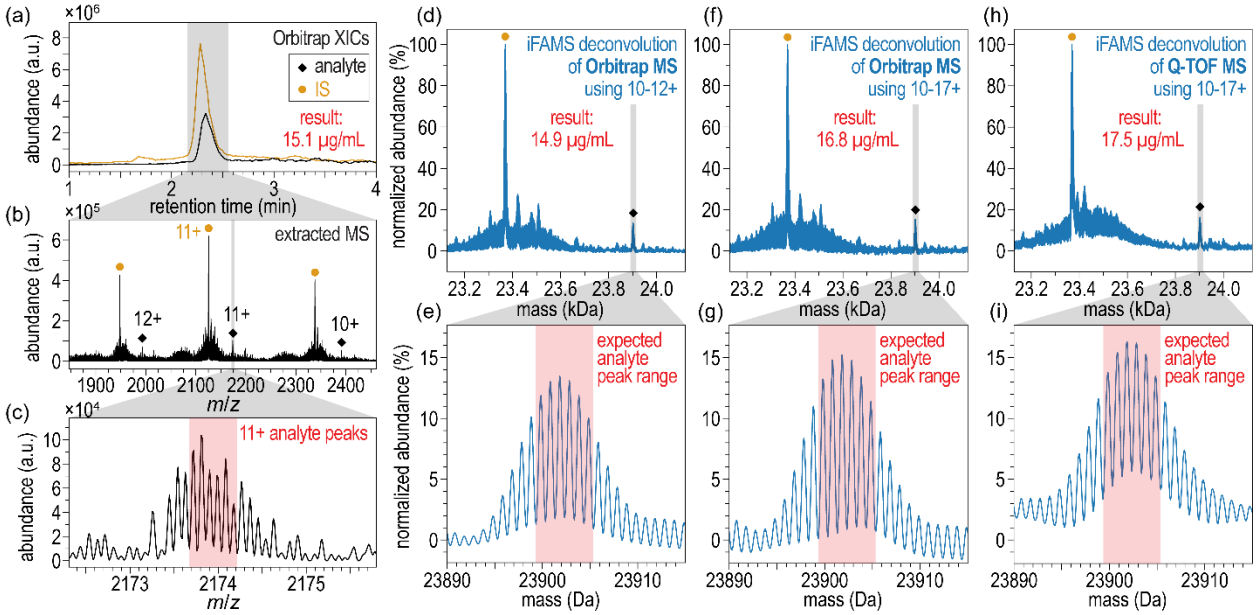

Figure S2. Example of good method agreement for subject sample analysis. (a) Extracted ion chromatograms (XICs) generated from the Orbitrap mass spectrum. The analyte XIC (black) was generated from charge states 10-12+, and the IS XIC (gold) was generated from charge state 11+. (b) Extracted mass spectrum (MS) from a 2.15-2.54 min retention time window zoomed in on the 10-12+ charge states. (c) MS zoom-in on analyte 11+ charge state with top six isotope peaks highlighted in red. (d) iFAMS deconvolution using charge states 10-12+ from the Orbitrap mass spectrum with analyte (black diamond) and IS peaks (gold circle) labeled. (e) Zoom-in on the analyte peak from the deconvolution in (d) with the top six isotope peaks highlighted in red. (f) iFAMS deconvolution using charge states 10-17+ from the Orbitrap mass spectrum with analyte (black diamond) and IS peaks (gold circle) labeled. (g) Zoom-in on the analyte peak from the deconvolution in (f) with the top six isotope peaks highlighted in red. (h) iFAMS deconvolution using charge states 10-17+ from the Q-TOF mass spectrum with analyte (black diamond) and IS peaks (gold circle) labeled. (i) Zoom-in on the analyte peak from the deconvolution in (h) with the top six isotope peaks highlighted in red.

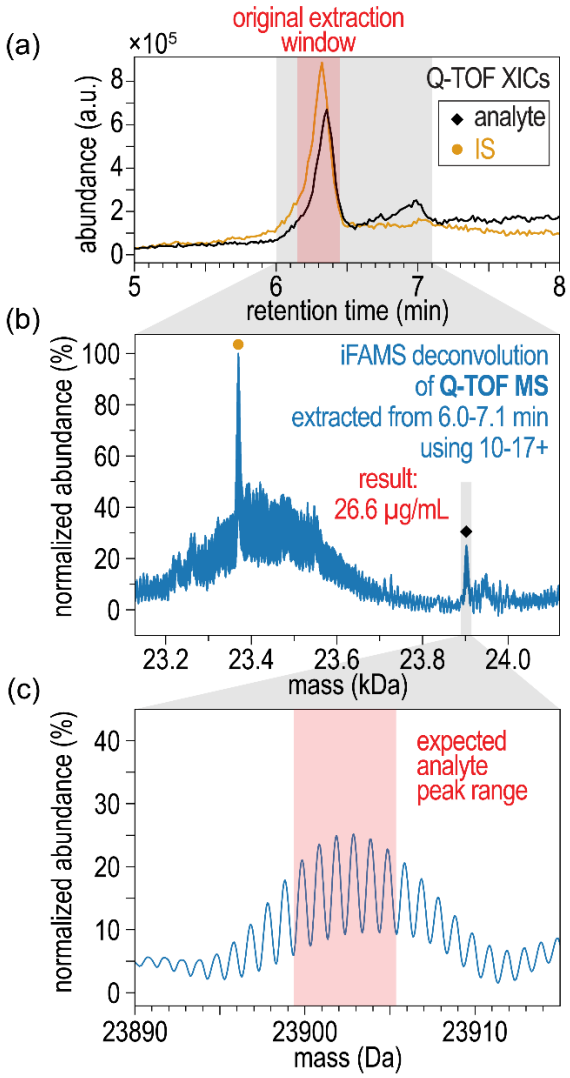

Figure S3. Drop in analyte signal example Q-TOF XICs and alternative deconvolution. (a) Extracted ion chromatograms (XICs) from the LC/Q-TOF data of a subject sample where a drop in calculated concentration was observed between Orbitrap and Q-TOF measurements. The analyte XIC (black) was generated from the six most abundant isotope peaks from each charge state included (10-12+). The IS XIC (gold) was generated from the six most abundant isotope peaks from the 11+ charge state. The red shaded region indicates the retention time window (6.15-6.45 min) used for extracting the mass spectrum for the original analysis. The gray shaded area indicates the retention time window (6.0-7.1 min) used for extracting the mass spectrum for the following deconvolution. (b) iFAMS deconvolution using charge states 10-17+ from the Q-TOF mass spectrum extracted from the wider retention time window with analyte (black diamond) and IS peaks (gold circle) labeled. (e) Zoom-in on the analyte peak from the deconvolution in (d) with the top six isotope peaks highlighted in red.

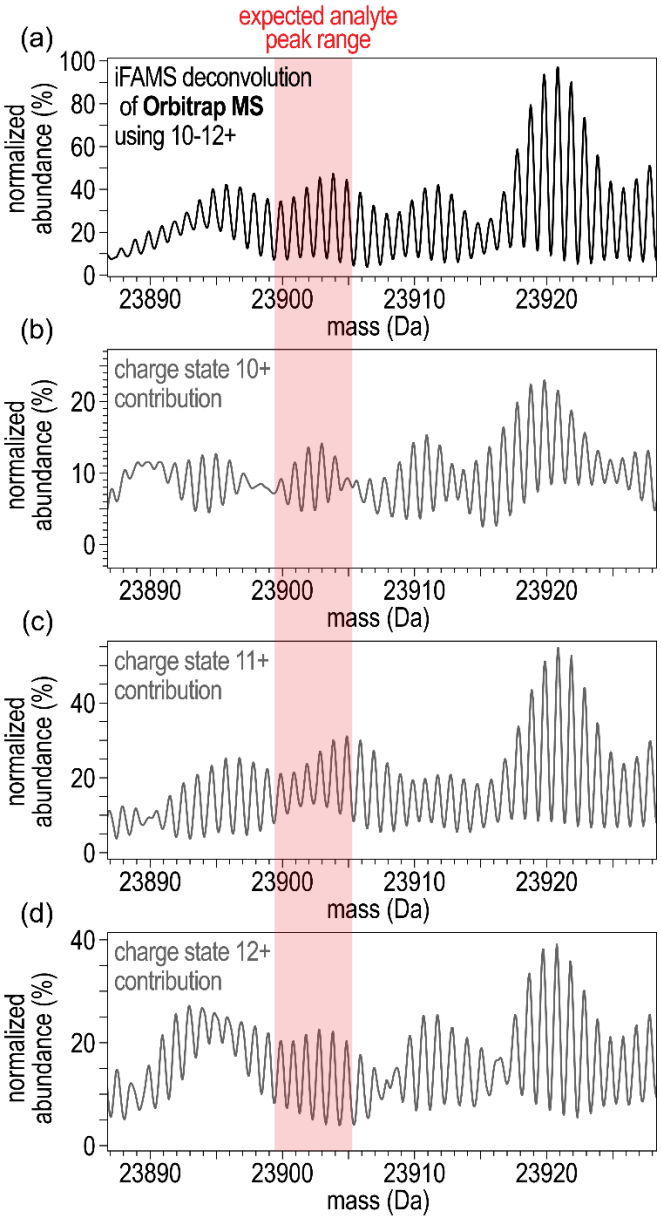

Figure S4. Individual charge state contribution to iFAMS deconvolution of Orbitrap MS with interferent. (a) Combined iFAMS Quant+ deconvolution of a subject sample with an interferent using charge states 10-12+ from the Orbitrap MS. Abundances are normalized to the most abundant feature within the window. The red highlighted region indicates the range of masses that the analyte is expected. (b) Contribution to the deconvolution from charge state 10+. (c) Contribution to the deconvolution from charge state 11+. (d) Contribution to the deconvolution from charge state 12+.